CONVECTION-REACTION EQUATION BASED LOW-FREQUENCY CONDUCTIVITY IMAGING USING READOUT GRADIENT INDUCED EDDY CURRENTS

Omer Faruk Oran[1], Fatih Suleyman Hafalir[1], Necip Gurler[1], and Yusuf Ziya Ider[1]
[1]*Electrical and Electronics Engineering, Bilkent University, Ankara, Turkey*

Introduction: Electrical conductivity has different values for different tissues of human body, and it also depends on the pathological state of the tissues. Besides, conductivity information would offer great advantages for the field of MR safety since specific absorption rate (SAR) is directly related to the conductivity. Several methods for imaging conductivity have been proposed. In Magnetic Resonance Electrical Impedance Tomography (MREIT), for instance, the magnetic flux density due to the current injected into the imaging object, is measured in the object using an MRI system, which is then used for the reconstruction of conductivity [1]. On the other hand, in Magnetic Resonance Electrical Properties Tomography (MREPT), B_1 field distribution, which is affected by the induced currents in Larmour frequency, is measured. This information is then used for the reconstruction of conductivity [2]. Since conductivity is a function of frequency of injected or induced current, MREIT and MREPT provide information about different parts of the conductivity spectrum, i.e. MREIT is for the very-low frequency range while MREPT is for the Larmour frequency. Recently, it has been proposed to utilize the eddy-currents induced by imaging gradients for conductivity imaging in kHz range and some current-density distribution images have been presented [3]. They have called this technique as Low Frequency-EPT, although we will refer as LF-MREPT. In this study, we derive the main equation for LF-MREPT which relates conductivity and induced current to the measured magnetic flux density and which is in the form of the well-known convection-reaction equation. Then we propose a LF-MREPT algorithm which is based on the solution of this equation. We also propose a method for reconstructing induced current density.

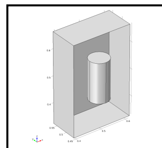

Fig 1. Simulation Phantom

Methods a) Measurement of B-field generated by induced currents due to imaging gradients: In MRI, during the rise-time of the readout gradient, the magnetic flux density can be decomposed as $\mathbf{B} = \mathbf{B}^p + \mathbf{B}^s$ where $\mathbf{B}^p$ stands for the primary B-field which is generated by the currents running on the gradient coil ($\mathbf{J}^p$) and $\mathbf{B}^s$ stands for the secondary B-field which is generated by induced eddy-currents ($\mathbf{J}^s$). The additional phase in MR complex images due to the z-component of $\mathbf{B}^s$ is given as $\int_0^{t_r} \gamma B_z^s(t)\,\mathrm{d}t$ where t_r is the rise-time of the gradient field and γ is the gyromagnetic ratio. Another complex image is obtained with reversed readout gradient polarity, and the phase difference of these images gives twice the additional phase while transceive and B_0 inhomogenity phase cancel out. Since B_z^s is approximately constant during the rise-time of the readout gradient, its distribution is obtained.

b) Reconstruction of induced currents due to readout gradient: For biological tissues at low-frequencies the Maxwell-Ampere equation is assumed to be $\nabla\times\mathbf{B}^s = \mu_0\mathbf{J}^s$ which may also be separately written for $\mathbf{B}^p$, $\mathbf{J}^p$ pair. Taking the curl of both sides and using the fact that $\nabla\cdot\mathbf{B}^s = 0$, the following relation is obtained: $\nabla\times\nabla\times\mathbf{B}^s = -\nabla^2\mathbf{B}^s = \mu_0\nabla\times\mathbf{J}^s$ **(Eq. 1)**. The z-component is given as $\frac{\partial J_x^s}{\partial y} - \frac{\partial J_y^s}{\partial x} = \nabla^2 B_z^s$ **(Eq. 2)** Using this equation and the Magnetic Resonance Current Density Imaging (MRCDI) algorithm of Park *et al* [4], J_x^s and J_y^s are reconstructed assuming $\partial J_z^s / \partial z \cong 0$.

c) Convection-Reaction Equation based LF-MREPT: Since $\mathbf{J}^s = \sigma\mathbf{E}$, Eq. 1 may be written as $-\nabla^2\mathbf{B}^s = \mu_0\nabla\times\sigma\mathbf{E} = \mu_0(\nabla\sigma\times\mathbf{E} + \sigma\nabla\times\mathbf{E})$ **(Eq. 3)** During the rise-time of the readout gradient (let's say x-gradient), $B_z^p = Kxt$ where K is the slew rate of the gradient field and thus $\partial B_z^p / \partial t = Kx$. Since Faraday's Law is $\nabla\times\mathbf{E} = -\frac{\partial\mathbf{B}^p}{\partial t} - \frac{\partial\mathbf{B}^s}{\partial t}$ and assuming $\frac{\partial B_z^s}{\partial t} << \frac{\partial B_z^p}{\partial t}$, the z-component of Eq. 3 becomes $\nabla^2 B_z^s = \frac{\mu_0}{\sigma}\left(\frac{\partial\sigma}{\partial x}J_y^s - \frac{\partial\sigma}{\partial y}J_x^s\right) + \mu_0\sigma Kx$ from which the key relation $\nabla\rho\cdot(-J_y^s, J_x^s) + \nabla^2 B_z^s\rho/\mu_0 - Kx = 0$ **(Eq.4)** is obtained where $\rho = \sigma^{-1}$ Eq. 4 may be recognized as the convection-reaction equation where ($-J_y^s$, J_x^s) and is identified as the convective field. Therefore advanced numerical methods which are already available for the solution of the convection-reaction equation may be used for solving Eq. 4. In our algorithm, finite element method (FEM) is used for the numerical solution of Eq.4. A similar algorithm has been previously proposed for MREIT where no reaction term exists [1].

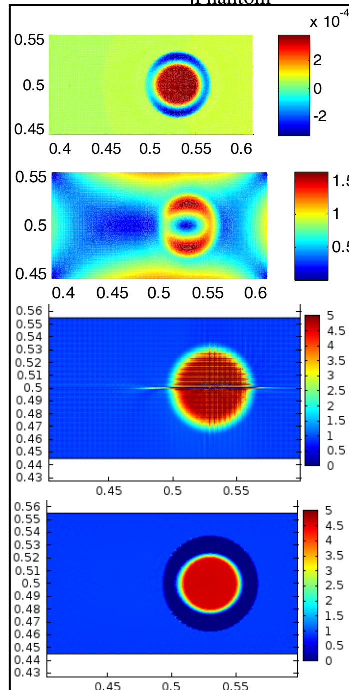

Fig 2. Top to bottom: a) $\nabla^2 B_z^s$ [T/m^2] b) Magnitude of the reconstructed current density [A/m^2] c) Reconstructed conductivity [S/m] d) Reconstructed conductivity when Eq.5 is used [S/m] .

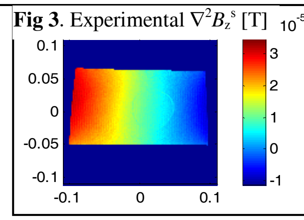

Fig 3. Experimental $\nabla^2 B_z^s$ [T]

Results and Discussion: In order to generate simulated B_z^s the phantom shown in Fig.1 is modeled and transient electromagnetic wave solution is obtained using Comsol Multiphysics (Comsol AB, Sweden). For simulations, gradient slew rate is taken to be K=500 T/m/sec. The background conductivity of the phantom (34×22.5×11cm) is 1 S/m while the cylindrical object (height 15 cm, ∅=7.5 cm) has conductivity of 5 S/m and the conductivity transition is not sharp but tapered. The simulated $\nabla^2 B_z^s$ for the central x-y plane is given in Fig 2a. As evident from Eq. 4, $\nabla^2 B_z^s$ changes linearly with respect to x at regions of constant conductivity. The magnitude of the reconstructed induced current is shown in Fig 2b. Since the convective field ($-J_y^s$, J_x^s) in Eq.4. consists of induced currents, the problem will be poorly defined in the regions the induced current is almost zero. For this reason, readout direction is changed to y and another data set is obtained so that the regions of zero convective field are shifted slightly. The matrices of x and y readout directions, which are obtained using FEM for solving ρ, are concatenated and the final matrix system is solved. The conductivity is successfully reconstructed as shown in Fig 2c. However, the artifact on y=0.5 line which is caused by low convective-fields in this region is still slightly present. On the other hand, in the regions where ρ slowly varies or is constant, the convection term (first term) in Eq. 4 can be neglected so that $\rho = Kx\mu_0/\nabla^2 B_z^s$ **(Eq. 5)** can be used for reconstruction. Using Eq. 5 in all regions, the conductivity distribution shown in Fig 2d is reconstructed. This conductivity reconstruction is successful in other than the conductivity transition region where ρ changes.

For experimental studies, we have built the phantom shown in Fig.1. A cylindrical container (filled with solution of 1 gr/l $CuSO_4$, 12 gr/l NaCl) is placed in a rectangular container (filled with solution of 1 gr/l $CuSO_4$, 6 gr/l NaCl). Two GRE images are obtained by using opposite readout gradient (x gradient is used) polarities (FOV: 220×220 mm, voxel size 1.72×1.72×5 mm, NEX:3, Gx=26.6 mT/m, tr=0.05 ms, K=Gx/tr=532 T/m/sec) using a 3T MRI Scanner (Magnetom Trio, Siemens, Germany). Measured B_z^s distribution is given in Fig 3. As expected B_z^s has a decreasing trend in the x-direction.

Conclusion: In this study, a convection equation based algorithm for LF-MREPT is proposed. We have shown by simulation results that the algorithm is successful. Preliminary experimental results show that B_z^s measurements are feasible. Since Laplacian operator amplifies the noise in B_z^s measurements, precautions should be taken when experimental data is used for reconstruction. We are currently working on reconstructing conductivity using experimental data.

Acknowledgements: This work is supported by TUBITAK 111E090 grant. Experimental data are acquired using the facilities of UMRAM, Bilkent University, Ankara.

References: [1] Oran et al, *Phys Med Biol*. 2012;57:5113-40. [2] Katscher et al, *IEEE Trans Med Imaging*. 2009;28(9):1365-74. [3] van Lier et al, *ISMRM 20* 2012:3467 [4] Park et al, *Phys Med Biol*. 2007;52:3001-13.